Multiscale Simulations of Heat Transfer and Fluid Flow Problems

Ya-Ling He

Wen-Quan Tao[1]
e-mail: wqtao@mail.xjtu.edu.cn

Key Laboratory of Thermo-Fluid Science and Engineering of MOE,
School of Energy and Power Engineering,
Xi'an Jiaotong University,
Xi'an, Shaanxi 710049,
People's Republic of China

The multiscale problems in the thermal and fluid science are classified into two categories: multiscale process and multiscale system. The meanings of the two categories are described. Examples are provided for multiscale process and multiscale system. In this paper, focus is put on the simulation of multiscale process. The numerical approaches for multiscale processes have two categories: one is the usage of a general governing equation and solving the entire flow field involving a variation of several orders in characteristic geometric scale. The other is the so-called "solving regionally and coupling at the interfaces." In this approach, the processes at different length levels are simulated by different numerical methods and then information is exchanged at the interfaces between different regions. The key point is the establishment of the reconstruction operator, which transforms the data of few variables of macroscopic computation to a large amount of variables of microscale or mesoscale simulation. Six numerical examples of multiscale simulation are presented. Finally, some research needs are proposed. [DOI: 10.1115/1.4005154]

Keywords: numerical approach, multiscale simulation, reconstruction operator, FVM, LBM, DSMC, MDS

1 Introduction

Multiscale simulation is a rapidly evolving area of research that will have a fundamental impact on applied mathematics and computational science and engineering. It is not an exaggeration to say that almost all problems have multiple scales in nature [1]. An ancient Chinese philosopher said: suppose you take a meter-long wood stick and cutoff half of it each day; you will never reach an end even after thousands of years! [2]. This is actually an excellent description of the multiscale nature of space.

Different physical laws may be required to describe the problem at different length and/or time scales. Taking the length scale of the fluid flow problems as an example, at the macroscale of fluids the continuum equation and the Navier–Stokes (NS) equations are the governing equations to accurately predict the density, velocity, and pressure fields. This is the continuum medium level or macroscale level. On the scale of the mean free path, however, the kinetic theory gives the description in terms of the one-particle phase-space distribution function, which is expressed by the well-known Boltzmann's equation. This may be regarded as the mesoscale level. At the nanometer scale, to predict the actual position and velocity of each individual molecule/atom that makes up the fluid, the Newton's law has to be used with a suitable potential function, which constitutes the microlevel. It should be noted that the inherent time scales for the above different length scale problems are also different [1]. The typical time scale for the continuum level is about second, while that at microlevel is around 10^{-12}–10^{-14} s.

Numerical simulation approaches at the level of a single scale have been rapidly developed in the past decade, and the methods for the continuum medium are in some sense becoming relatively mature, for example, the finite volume method (FVM) for the fluid flow and heat transfer [3–8]. In addition, methods in mesoscale level, i.e., the lattice Boltzmann method (LBM) [9–13] and the direct simulation of Monte Carlo method (DSMC) [14,15] have also been rapidly developed. LBM and DSMC belong to the mesoscale class: these two methods adopt a concept of computational particles, which are much larger than an actual molecule but act as a molecule (simulation molecule). For example, in DSMC a computational particle may be a representative of a collection of 10^6–10^{11} molecules [16,17]. In molecular dynamics simulation (MDS) every molecule is simulated according to the Newton's law of motion [18–20]. The major advantage of MDS is that it does not need to input phenomenological descriptions such as constitutive equation [21] and the thermophysical properties as that for the macrotype method. One thing is common to the three methods (LBM, DSMC, and MDS) that the macroparameters (such as velocity and pressure) are obtained via some kinds of statistical average. The numerical methods at the three scales and their related physical and mathematical descriptions are illustrated in Fig. 1 [22].

In spite of the tremendous successes achieved in the above three levels of numerical approaches, they have their own limitations. For the macrotype numerical approach (finite difference method (FDM), (FVM), and finite element method (FEM)), the major limitation is the complete neglect of microscopic mechanism and hence the introduction of some empirical or ad hoc assumptions, including empirical parameters. On the other hand, the mesoscale or microscale method, even though can reveal the details of a complex mesoscale or microscale process, they usually require enormous computer memory and computational times. Hence, the size of their computational domain is heavily restricted, especially the methods of DSMC and MDS. For example, the space size that MDS can work at the present computer hardware, say, a modern work station is usually in the order of tens of nanometers, and the time scale is about 10^{-10}–10^{-12} s. If the MDS is adopted to simulate an entire engineering heat transfer or fluid flow process, the required memory and CPU times are truly prohibited. Concerning the mesoscale methods, although DSMC and/or LBM are orders of magnitude faster than molecular dynamics for simulation of gases or liquids, it is orders of magnitude slower than the continuum algorithms for solving partial differential equations of aerodynamics or hydrodynamics in the Navier–Stokes limit. One very useful approach that may be applied to some engineering problems is: only flow regions that require molecular resolution are treated by MDS, where the atomic-scale dynamics is important, DSMC/LBM are adopted for regions, which require mesoscale resolution, and a macroscopic

[1]Corresponding author.

Contributed by the Heat Transfer Division of ASME for publication in the JOURNAL OF HEAT TRANSFER. Manuscript received September 11, 2010; final manuscript received August 4, 2010; published online January 19, 2012. Assoc. Editor: Jungho Kim.

 Copyright © 2012 by ASME

Downloaded From: http://heattransfer.asmedigitalcollection.asme.org/ on 03/05/2013 Terms of Use: http://asme.org/terms

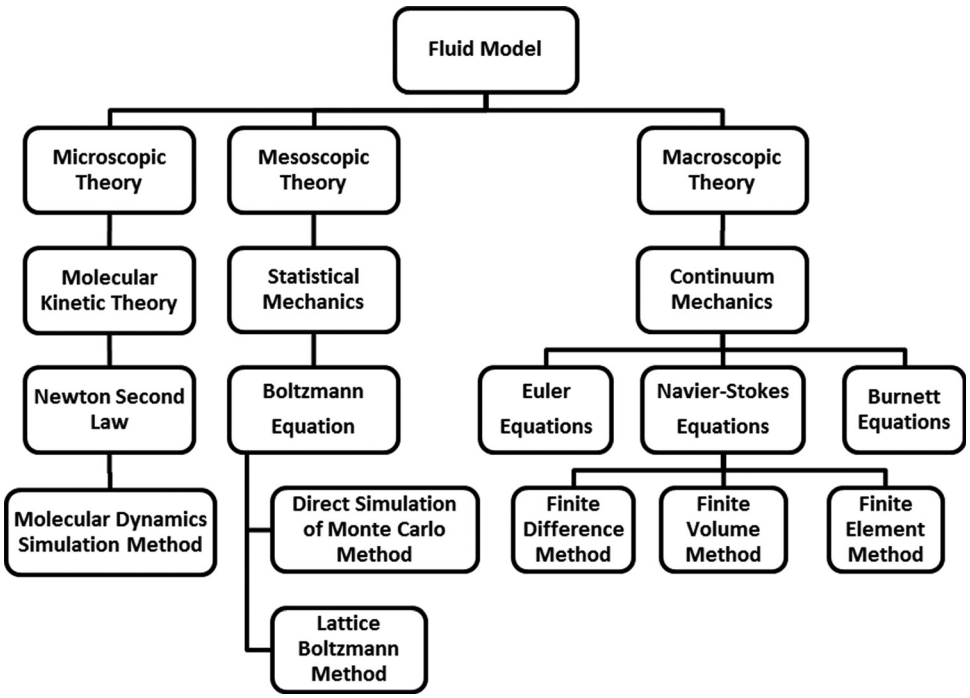

Fig. 1 Numerical approaches at three geometric scales and their related physics

numerical method everywhere else. This is where the idea of multiscale simulation (modeling) comes in, and it has been widely adopted in the material science for about 10 years and great achievements have been attained [23–25]. In the following, we will take some examples in heat transfer and fluid flow to further illustrate the above idea.

From engineering computation point of view multiscale problems in the thermal and fluid science and engineering may be classified into two categories: multiscale process and multiscale system [26]. Four examples are presented below for the multiscale process.

Turbulent flow is a typical example of multiscale process, which involves many different length scales of eddies. Recently, well-developed direct numerical simulation (DNS) of the turbulent flow can resolve all kinds of eddies in details [27]. In this paper, turbulent flow is only taken as an example of multiscale process but will not be further discussed from the point view of multiscale simulation. The launching process of a space craft provides another example where the fluid flow around the spacecraft experiences different gas flow regimes and different numerical approaches should be used in different regimes in order to make the numerical simulation efficient. It is well-known that gas flow regimes can be classified according to its Knudsen number, which is defined as

$$\mathrm{Kn} = \frac{\lambda}{L} \tag{1}$$

where λ is the mean free path of the molecules and L is the characteristic geometric length of the flow domain. Mean free path is an important parameter in gas kinetics, which means the average length of track between two successive molecule collisions. Based on Kn, gas flow is classified into four regimes [28,29]: continuum flow ($\mathrm{Kn} < 0.001$), slip flow ($0.001 < \mathrm{Kn} < 0.1$), transition flow ($0.1 < \mathrm{Kn} < 10$), and free molecule flow ($\mathrm{Kn} > 10$). In Fig. 2, the application feasibility of the numerical methods at three levels is schematically presented for gas flow predictions.

The third example is the transport process in a proton exchange membrane fuel cell (PEMFC), where the fuel gas flow in polar plate channels occurs at the length scale of centimeters, the diffusion process in the gas diffusion layer and the transport of proton in the membrane occur at the order of hundreds of micrometers, while the reaction in the catalyst happens in a thickness of tens or even several micrometers (Fig. 3). The electrochemical reaction and transport process in the catalyst layers in turn are highly complex multiscale phenomena. In this layer, reactants are transported through void pores and electrolyte in catalyst layer, the characteristic length of which is in the range of 10–100 nm. The catalyst particles are randomly distributed in this layer with a diameter of several nanometers [30]. Numerical simulation is widely adopted in the study of PEMFC, and at present stage most numerical simulations are based on macroscale approach, such as FVM. In literatures, many numerical simulation results are often compared with the same tested U-I output curve (say, Refs. [31] and [32]) with a number of empirical parameters. The number of such parameters is often larger than ten. For example, in a 3D, two-phase, nonisothermal model 14 empirical parameters are involved [33,34]. It is found that the effects of these parameters on the U-I output curve may be qualitatively different. Thus, even though the values adopted for the empirical parameters are quite different, the simulated output curves from different authors are often claimed being in a good agreement with the same test curve. We once obtained two almost the same U-I output results with two sets of empirical parameters [33]. To completely discard such unpleasant situation, the only approach is probably to develop a multiscale simulation model in which macroscale, mesoscale, and microscale/nanoscale simulations are used for different regions and information is exchanged at the interface.

Condensation of refrigerant vapor on enhanced surface of a tube serves the fourth example where multiscale simulation is needed in order to make an actual full simulation. In 1974 Hitachi in Japan developed an enhanced structure for refrigerant vapor condensation, Thermoexcel-C [35]. Since then 37 years has past, what kind of achievement has been made as far as numerical performance prediction for such kind of phase change enhanced surface is concerned? Although a number of enhanced structures have been developed to meet different requirements or conditions, it is almost nothing in the advances of numerical prediction! We still heavily rely on experimental measurements for obtaining the performance of different enhanced surfaces. Technicians have to measure the geometry in details via an industrial microscope (Fig. 4) in order to collect useful information for further improvement.

Downloaded From: http://heattransfer.asmedigitalcollection.asme.org/ on 03/05/2013 Terms of Use: http://asme.org/terms

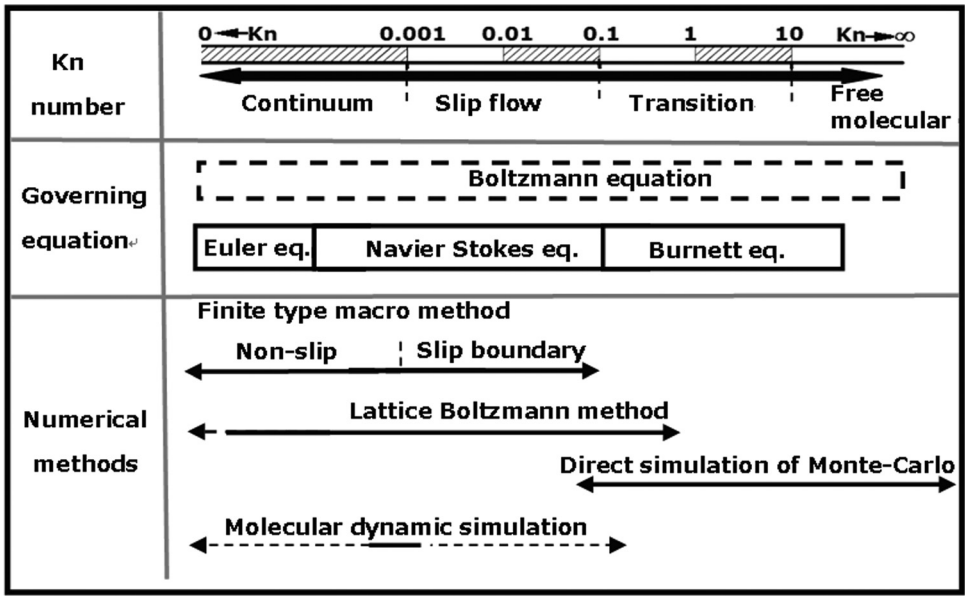

Fig. 2 Application feasibility of different level numerical methods

It is our understanding that only the multiscale simulation can solve this problem where the MDS is used to simulate vapor condensation on a complicated surface; the LBM (FVM) is adopted to simulate the fluid flow in the condensed film; and FVM for the temperature field in the solid wall.

Now attention is turned to the multiscale system. By multiscale system, we refer to a system that is characterized by large variation in length scales in which the processes at different length scales often have the same governing equations and are not so closely related as in the first category. The cooling of an electronic system is such a typical multiscale system [36–38]. The length scale variation of a data center from the interconnects of a chip to room is about 11 orders, and that from a chip to a cabinet has at least three or four orders. In Refs. [37] and [38], a top-to-down sequential multilevel simulation method with increasing fineness of grids was proposed. Since the simulation methods at the different levels in such multiscale system are all continuum type and [37,38] have given clear presentation, the numerical method for the multiscale system will not be further discussed in this paper. In the following presentation attention will only be paid for the simulation of multiscale process.

Study on the multiscale process may be conducted from mathematical point of view and from engineering point of view with different emphasis. As indicated in Refs. [39] and [40], there is a long history in mathematics for the study of multiscale problems. From mathematical point of view, mathematical methods, such as multigrid techniques, domain decomposition, adaptive mesh refinement, and coarse-grained Monte Carlo models are all belong to multiscale techniques [39,40]. It seems that from mathematical point of view the terminology "multiscale" is referred to a numerical method for solving a physical problem, which involves grids with a significant difference in geometrical scales. Multigrid technique for solving algebraic equations is a typical such numerical method. In this paper for the numerical simulation of the multiscale process, the word "scale" is used in such a sense that phenomena in different scales have different governing equations or descriptions. From this point of view, the multigrid method will not be referred to as a multiscale technique, since it is used to solve the algebraic equation discretized from governing equations at the macroscopic level. The present authors believe that such an understanding is physically more meaningful, more agreeable to the picture shown in Fig. 1, more consistent with our statement: "This is where the idea of multiscale simulation (modeling) comes in" mentioned above, and hence it can be regarded as the physical (engineering) point of view.

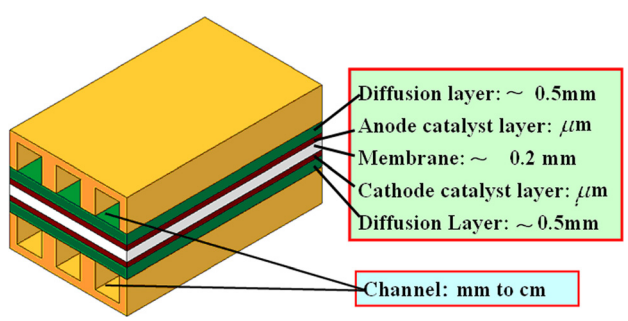

Fig. 3 Multiscale transport process in PEM fuel cell

2 Major Numerical Approaches for Simulating Multiscale Process

For the numerical modeling of multiscale processes in engineering thermal and fluid science, two types of numerical approaches may be classified. They can be described as: (1) "Using uniform governing equation and solving for the entire domain"(2) "Solving problems regionally and coupling at the interfaces." The DNS is a typical example of the first numerical approach [27]. Another example of the first approach is the simulation of gas flow in different ranges of Knudsen number by using Boltzmann equation, as suggested by Li and Zhang [41]. In their paper, the Bhatnagar-Gross-Krook (BGK) model was modified and some special techniques were introduced. A unified numerical scheme for solving gas flow from rarefied to continuum is then established. This numerical approach is attracting, however, as indicated above and will be shown later that for continuum flow, the macroscopic methods are orders faster than mesoscale methods. Even though coupling process will take some more time, but as a whole the multiscale method will be computationally more efficient [42]. This implies that when the macroscale method works it should be the first candidate. The mesoscale/microscale methods should be used for such cases when the macroscale methods fail to work or do not work efficiently. Thus, we will not go further for the approach of using uniform governing equation and solving for the entire domain. In the following focus will be put on the second approach.

The second approach is the most widely used one. In this approach, the process at different length levels is simulated by

Downloaded From: http://heattransfer.asmedigitalcollection.asme.org/ on 03/05/2013 Terms of Use: http://asme.org/terms

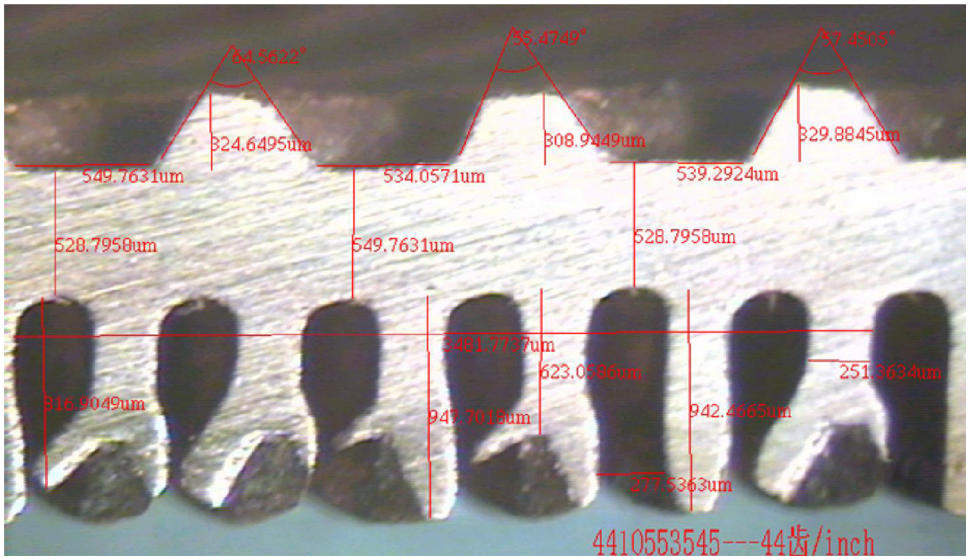

Fig. 4 Cross section of an enhanced surface viewed from an industrial microscope (magnified by ten times)

different numerical methods and then information is exchanged at the interfaces of different regions. Mathematically this solution approach is quite similar to the domain decomposition method in solving partial differential equations [43], which was originated from Schwarz alternative method [44]. If the exchange of information at the interface ("hand-shaking" region) is performed via Dirichlet type, then it can be mathematically expressed by

$$U = \mathbf{C}_{\mathrm{D}} u; \quad u = \mathbf{R}_{\mathrm{D}} U \tag{2a}$$

where U and u are the macroscopic parameter and microscopic/mesoscopic parameter, respectively. $\mathrm{C_D}$ and $\mathrm{R_D}$ are the Dirichlet compression and reconstruction operators, respectively. The information at mesoscale or microscale level may be transferred to the macroscale level via Neumann type, that is, by supplying flux at the interface, then we have

$$q = \mathbf{C}_{\mathrm{N}} u; \quad u = \mathbf{R}_{\mathrm{D}} U \tag{2b}$$

where q is the interface flux of the continuum region.

At the interface between different regions, there will be a mismatch in the kind and number of variables used by the different regions. The Dirichlet compression operator $\mathrm{C_D}$, which extracts the macroscopic parameters from a large amount of data at microscale or mesoscale level by some averaging or integrating principles, is easy to be defined, but the reconstruction operator $\mathrm{R_D}$, which should prolong small amount of macroscopic parameters into a large amount of parameters at mesoscale or microscale is quite difficult to be constructed. Here, we meet a one-to-many problem since the macroscopic variables have to be mapped to more LBM (DSMC or MDS) variables. The design of the compression and reconstruction operators should abide by some basic physical laws or principles, such as mass conservation, momentum, and energy conservation. In addition, the operator should be mathematically stable, computationally efficient and easy to be implemented. In a word, the exchange of information should be conducted in a way that is physically meaningful, mathematically stable, computationally efficient, and easy to be implemented. It should be noted that by the terminology "operator" we mean: (1) It is an actual mathematical formula for transferring (converting) results of different regions at the interface; or (2) It is a set of numerical treatments for transferring information, which are developed from some fundamental considerations. At the present, the second one is the most frequently encountered situation.

In the following some existing coupling principles, basically Dirichlet reconstruction operator, between any two of the three scale methods are presented.

2.1 Coupling Between MD and FVM (FDM and FEM). In 1995 O'Connel and Thompson [21] proposed a way for coupling the simulation by MDS and FDM. This is the first paper in the literature initiating the coupled MDS-macroscale simulation. In their paper, the coupling is achieved by constraining the dynamics of fluid molecules in the vicinity of the MDS-continuum interface to meet the requirement of mass and momentum continuity. The different solution regions are shown in Fig. 5, where the interface is referred to as hybrid solution interface (HSI). The MDS portion of the computation is beyond the HSI (shown by the open circles), introducing an overlap region. Continuity of mass flux at the HSI is achieved by supplying the velocity boundary condition for the continuum region by the averaging results of the MDS over the zero bin shown in Fig. 5. Ensuring the momentum conservation in the HSI region is a more subtle issue because as indicated above in the MDS simulation there is not any constitutive equations for stress. In order to ensure the continuity of momentum (stress), it is required that in the overlap region within any bin shown in Fig. 5, following constraint should be satisfied:

$$\sum_{n=1}^{N_j} p_n - M^{(j)} v_x^{(j)} = 0 \tag{3}$$

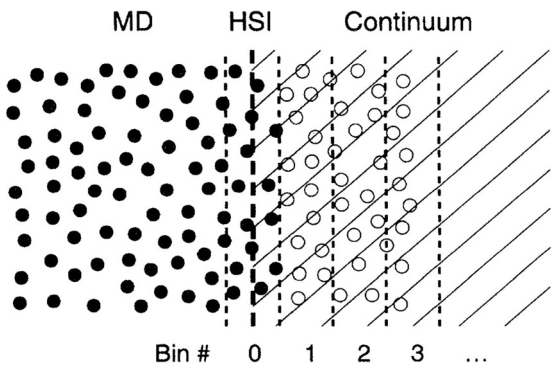

Fig. 5 Schematic for the coupling between MD and continuum method [21]

Downloaded From: http://heattransfer.asmedigitalcollection.asme.org/ on 03/05/2013 Terms of Use: http://asme.org/terms

where N_j is the total number of molecules in the jth bin and p_n is the momentum of the nth molecule in the x direction, $M^{(j)}$ denotes the mass of the continuum fluid element corresponding to the jth bin, and $v_x^{(j)}$ is the velocity. Obviously, Eq. (3) requires that in the jth bin the x-direction momentum computed from microscale and macroscale results should be identical. By integrating this equation with time, a holonomic constraint can be obtained and it is incorporated into Lagrange's equation for any molecule in the jth bin. This constraint is implemented for all the molecules in the bins within the overlap region, thus the momentum conservation requirement is fulfilled.

Since this pioneering work a number of MDS-continuum coupling researches have been published for different flow and heat transfer cases with focus being put on the improvement of coupling stability, accuracy, and efficiency. Nine examples related to multiscale simulation of heat transfer and fluid flow problems since 2000 can be found in Refs. [45–53] as the representative results. The details in the improvements of coupling methods are not stated here because of space limitation and can be found in the above-referenced paper.

2.2 Coupling Between DSMC and FVM (FEM). There are two kinds of coupling of DSMC-continuum, i.e., fluid-to-fluid and fluid-to-solid. Attention is first put on the fluid-to-fluid coupling. This DSMC-continuum coupling is for the prediction of gas flow composed of different flow regimes. As shown by Eqs. (2a) and (2b), information may be transferred by variables themselves (Dirichlet type) or by their fluxes (Neumann type). According to Ref. [54] when convert the DSMC results to macroscopic parameters, the Neumann boundary condition may cause large statistical error, especially under the condition that the boundary is parallel to the flow direction, so the Dirichlet type transfer is often used for the DSMC-continuum information exchange [55].

In the coupled computation of DSMC and the NS via FVM or FEM one important issue is the determination of the location of breakdown interfaces between continuum and rarified gas regions. One practice is to specify the breakdown location in advance and the structured grid system is used in the continuum region [55,56]. The disadvantage of such a practice is that the prespecified breakdown interface does not follow faithfully the interface determined by some criteria, which may in turn either increase the computer run time or decrease the solution accuracy [57]. Recently, Wu et al. [55,58] proposed a parallel hybrid DSMS-NS scheme using 3D unstructured mesh with dynamic determination of the breakdown location in the continuum region by FVM. In the paper, the continuum conditions are marked by the local Kn which can be defined by the following general formula:

$$\mathrm{Kn}_{GL-Q} = \frac{\lambda}{Q_{\mathrm{local}}}|\nabla Q| \tag{4}$$

where Kn_{GL-Q} is the gradient-length Knudsen number; Q is the specific flow property, which can be the local density ρ, or local temperature T or local velocity $|V|$, and $Q_{\mathrm{local}}/|\nabla Q|$ is the general local characteristic length. The maximum of the local Kn obtained from density, temperature, and velocity is taken as the local Kn. That is

$$\mathrm{Kn}_{GL} = \max(\mathrm{Kn}_{GL-\rho}, \mathrm{Kn}_{GL-T}, \mathrm{Kn}_{GL-|V|}) \tag{5}$$

If the thermal equilibrium condition is taken into consideration, the above equation can be related to the translational temperature and the rotational temperature of the gas. For the details [59] can be referred. Usually, the interface region is allocated in the area where $0.02 < \mathrm{Kn}_{GL} < 0.04$.

Then, the overlapping regions between DSMC and NS solver are determined. The major idea is quite similar to that shown in Fig. 5 for the coupling of MD and continuum method. Between the regions where DSMC and NS solver are individually used, there is some overlapping region in which both DSMC and NS solver are adopted, and it is in this overlapping region the transfer of the Dirichlet boundary condition for NS solver from previous computation of DSMC and that for DSMC from previous NS solution is conducted.

Obviously, the solution procedure of such DSMC-continuum coupling is iterative in nature. For the details [55] can be consulted.

For the Dirichlet–Neumann type information exchange Ref. [60] can be referred.

Attention is now turned to the fluid–solid coupling. The gas flow in a micronozzle is often in the regions of transitional or free molecule and in this case coupling of the rarified gas flow with the heat conduction in the nozzle wall may occur. Traditionally, surface temperature of flow field was all set up before calculation and assumed that it was constant during the simulation process [61–65]. But in fact, it is very difficult to set up wall temperature reasonably prior to computation. In Refs. [66] and [67], coupled thermal-fluid methods were developed to simulate the time-dependent performance of high temperature micronozzle. The flow field characteristics were obtained by DSMC method, and the solid area temperature distribution was calculated by finite element method. Dirichlet—Neumann transfer method was used to couple the temperature obtained by FEM and heat flux obtained by DSMC method at the boundary. The whole unsteady process from starting up to temperature reaching melting point of silicon was simulated, so it was very time-consuming and computationally expensive. In Ref. [68], a DSMC-FVM coupled simulation for the rarefied gas flow in a FMMR was conducted. The Dirichlet–Neumann transferring method is used to couple the temperature and heat flux at the boundary of flow field and solid area. The implementation process is as follows. First, the wall surface temperature is set up and then DSMC simulation is executed, so the heat flux can be calculated from the flow field, and this heat flux is used as the boundary condition for the temperature field of the solid area including the wall surface. The temperature field in the solid area is obtained by solving the heat conduction equation by the FVM with unstructured grid system. The wall surface temperatures are thus updated and used as the boundary condition for the flow field solved by DSMC. Such steps are repeated until steady state has reached. Once steady state has reached, the solid temperature will not be calculated any more, namely, the surface temperature of fluid area is kept constant, but DSMC procedure in the fluid is continued. The sampling of macroparameters with each cell should be performed for a long time period in order to minimize statistical scatter. It is interesting to note that all boundaries of the nozzle in Ref. [68] are of second kind. It is well-known in heat conduction theory that such boundary conditions will lead to a temperature distribution with fixed gradient but cannot fix the absolute values. The energy conservation principle is used to fix the temperature distribution of the nozzle wall, namely, when the converged temperature solution of the nozzle wall is approached, the net heat transfer of the nozzle wall with the gas around it should be zero. Due to the low density of the propellant, the heat flux is very small, so there is a little temperature change in solid area during every time step. It would take a long time to arrive at steady state, which means that the time-marching of the unsteady state process in solids is computationally expensive. Considering that the time scale of flow area is much less than the time scale of solid area. A steady-state solution of gas flow is first obtained, and the DSMC results are used to update the wall boundary condition. An overrelaxation method is adopted in the solution process of heat conduction equation that accelerates the convergence but does not influence the steady-state temperature distribution in the solid region. Partial results of this work will be presented in Sec. 3.3.

2.3 Coupling Between LBM and FVM (FDM and FEM). As indicated above, LBM is a kind of mesoscopic methods, which sits between the macroscale and microscale levels, and this feature has been vividly described in Ref. [69] as "The LBE could

Downloaded From: http://heattransfer.asmedigitalcollection.asme.org/ on 03/05/2013 Terms of Use: http://asme.org/terms

potentially play a twofold function—as a telescope for the atomistic scale and a microscope for the macroscopic scale." In Ref. [69], an attempt is even made to adopt LBM more than one physical scale of description—from atomistic, kinetic, and to continuum fluid. Even though two examples were presented in Ref. [69], we would rather consider LBM as a mesoscale method. As indicated above, LBM is computational expensive compared with FVM and it should be used where the continuum methods cannot work effectively, for example, flow through a porous media. Thus, study on the coupling between LBM and continuum method is meaningful.

The coupling of FDM with LBM was conducted in Refs. [70] and [71], but the coupling computations were only implemented for the solution of one dimensional diffusion equation. A general coupling scheme, or a general reconstruction operator for transferring information from macroscale results to mesoscale parameters for multidimensional fluid flow is highly needed. Mathematically such transforming relation is called "lifting relation" which means that macroscopic variables in a low degree-of-freedom (DoF) system are upscaled to the macroscopic variables in a high DoF system. As indicated above, it is difficult to establish the one-to-one map from a low DoF system to a high DoF system. In Refs. [72] and [73], a reconstruction operator for the density distribution function of LBM has been derived based on multiscale perturbation approach. According to the derivation, the density distribution function of LBM, f_i, can be expressed from the macroscale parameter as

$$f_i = f_i^{(eq)}\left[1 - \tau\Delta t U_{i\beta}c_s^{-2}\left(U_{i\alpha}\partial_{x_\alpha}u_\beta + \nu\partial_{x_\alpha}^2 u_\beta + \nu\rho^{-1}S_{\alpha\beta}\partial_{x_\alpha}\rho\right)\right] \tag{6}$$

where $f_i^{(eq)}$ is the equilibrium density distribution function; c_s is the lattice sound speed; $S_{\alpha\beta}$ is the stress tension in α, β coordinates; τ is the nondimensional relaxation time; Δt is the time step; ν is the kinematic viscosity; ρ is the fluid density; $U_{i\alpha} = c_{i\alpha} - u_\alpha$, and u_α is the velocity in α direction; $S_{\alpha\beta} = \partial_{x_\beta}u_\alpha + \partial_{x_\alpha}u_\beta$.

In Refs. [22] and [74], a reconstruction operator for the temperature distribution function of the thermal lattice Boltzmann model is derived based on the same approach, it reads

$$F_i = F_i^{(eq)}\left\{1 - \tau'\Delta t T^{-1}\left[U_{i\alpha}\partial_{x_\alpha}T + a_T\left(\partial_{x_\alpha}\right)^2 T\right]\right\} + \frac{\tau'\omega_i T c_{i\beta}}{\tau U_{i\beta}}\frac{\left(f_i - f_i^{(eq)}\right)}{f_i^{(eq)}} + \tau'\Delta t\omega_i c_{i\beta}T\rho^{-1}\partial_{x_\beta}\rho \tag{7}$$

where F_i is the temperature distribution function, a_T is thermal diffusivity, τ' is the temperature relaxation time, Δt is the time step, and T is the temperature.

Equations (6) and (7) are general analytic expressions for reconstructing the microvariables of density and temperature distribution functions from the macrovariables. Their applications will be illustrated later.

2.4 Coupling Between MDS and LBM. In Ref. [75], an interesting numerical simulation was conducted for flow in nanoduct by using both MDS and LBM. The major purpose is to see if the space and time steps of LBM were fine enough. The results show that when the LBM space step is of 0.25σ, the velocity distributions from LBM are quite consistent with those of MDS, while the computation time of LBM is only about $1/1000$ of MDS. This study demonstrates that a spatial hand shaking between LBM and MDS is possible. According to this paper to couple LBM with MDS, the grid of LBM should has its finest scale $\Delta x_{\text{fine}} \sim \sigma$ near the coupling boundaries, and then progressively increases the mesh size so as to reach a 100-fold larger mesh spacing in the bulk flow. In Ref. [76] coupling LBM and MDS for liquid argon past a carbon nanotube was conducted. The LBM and MDS communicate via the exchange of velocities and velocity gradients at the interface. It is worth noting that a more efficient way is taking statistically averaged value from the results of MDS and using Eq. (6) to get density distribution function for LBM, and taking the integrated results of LBM as the macroparameters for MDS. In such a way, the smallest grid in LBM region needs not to be so fine as can be compared with σ. An example from authors' practice will be provided later.

It should be noted here that in this paper by "coupling" or "coupled" we mean that the computational domain is decomposed, and numerical methods at different scale levels are used in different subregions with information exchanging at the interfaces to make consistency of the solution in entire domain. In literature sometimes coupled methods may imply that the flow fields are solved by LBM and the governing equations for other scale variables are solved by FVM (FDM, FEM) [77]. Such coupling is not the content of this paper.

3 Examples of Multiscale Simulation

3.1 Coupling of MDS and FVM for Flow in Nanochannels With Roughness. The liquid flow in nanochannels with roughness is studied using the multiscale hybrid simulation in Ref. [78]. The computational domain is decomposed into particle, continuum, and overlap regions, where molecular dynamics, finite volume method, and coupling method are applied correspondingly (Fig. 6). In the main flow area, the FVM is employed as C solver. In the boundary vicinity, the classical MD simulation is used as P solver. In order to ensure the parametric continuity, the coupling method is needed for the O region. Since the flow condition is absolutely symmetric about the central line, the actual computational domain is chosen the half channel.

The P region size is $l_x^{\text{P}} = 25.4\sigma$, $l_y^{\text{P}} = 6.8\sigma$, $l_z^{\text{P}} = 40.7\sigma \sim 81.4\sigma$. 3D MDS is carried out with the modified Lennard–Jones (L-J) potential describing the interaction between liquid molecules by Ref. [79]

$$\varphi(r) = 4\varepsilon\left\{\left[\left(\frac{\sigma}{r}\right)^{12} - \left(\frac{\sigma}{r}\right)^{6}\right] + \left(\frac{r}{r_c}\right)^2\left[6\left(\frac{\sigma}{r_c}\right)^{12} - 3\left(\frac{\sigma}{r_c}\right)^{6}\right] - \left[7\left(\frac{\sigma}{r_c}\right)^{12} - 4\left(\frac{\sigma}{r_c}\right)^{6}\right]\right\} \tag{8}$$

where σ and ε are the length and energy characteristic parameters, and the cutoff radius $r_c = 2.5\sigma$. The interaction between solid and liquid is also described by Eq. (8), but the characteristic parameters are changed into $\sigma_{\text{wf}} = 0.91\sigma$ and $\varepsilon_{\text{wf}} = \beta\varepsilon$, where β is set to adjust the strength of the liquid–solid coupling. The simulated fluid is argon ($\sigma = 0.3405$nm and $\varepsilon = 1.67 \times 10^{-21}$J).

The time step for P region is $\delta t^{\text{P}} = 0.005\tau$ ($\tau = m^{1/2}\sigma\varepsilon^{-1/2}$). The simulation procedure contains two periods for each run, i.e.,

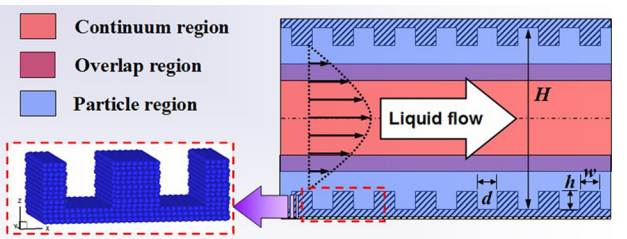

Geometric conditions

d(σ)	w(σ)	h(σ)	h/H(%)		
			H=122 σ	H=183 σ	H=244 σ
3.36	3.36	3.32	2.72	1.81	1.36
6.71	6.71	6.64	5.44	3.63	2.72

Fig. 6 Schematic of the hybrid simulation in a nanochannel with roughness

Downloaded From: http://heattransfer.asmedigitalcollection.asme.org/ on 03/05/2013 Terms of Use: http://asme.org/terms

equilibrium and coupling periods. Equilibrium period is the initial 250τ, during which the molecules in P region reach the thermal equilibrium state at $T_w = T_g = 1.1\varepsilon k_B^{-1}$. Coupling period is the next 5000τ, during which the coupling method is executed to ensure the synchronization between P and C regions.

The computational size for C region is divided by uniform grids $\Delta x^c = \Delta z^c - l_x^P$. The SIMPLEC algorithm is employed to solve the flow and pressure fields.

Some simulation results are now presented. In Fig. 7(*a*), the velocity distribution for a roughened channel is presented. It can be clearly observed that the fluid velocity at the wall keeps zero due to the obstacle of roughen element, causing a locking boundary condition, which is quite different from the case with smooth surface in which the velocity slip will occur (see Fig. 7(*b*)).

3.2 Flow Past a Nano-Tube by Coupling of MDS and LBM. Coupled simulation of MDS and LBM for flow past a nanotube is provided in Ref. [76]. Figure 8 shows the computational domain and the details of the three regions: center part around the nanotube is simulated by MDS, the far-outside by LBM, and the middle between the two regions is a hand-shaking area where both MDS and LBM are used. Macrovelocity is obtained from MDS and by using the reconstruction operator; density distribution function is obtained and serves as LBM boundary condition (along the dotted line of Fig. 8(*b*)). Particles velocities are given by a Maxwellian distribution with mean and variance consistent with the LBM results (in the shaded area of Fig. 8(*b*)). Simulation results are presented in Fig. 9 with the results from Ref. [76] for the same problem. It can be seen that the u velocities at the two center lines from the two numerical methods agree with each other quite well, while the coupled MDS and LBM gives more smooth stream function distribution. In this coupled simulation by both LBM and MDS one may argues how far does one need to extend the MD region to achieve accurate results. According to Ref. [80], given a fixed sampling period in each iteration of coupled method, there exists an optimal size of the MDS region considering both the computational efficiency and accuracy. The size of the MDS region of Ref. [81] is nearly optimal after some preliminary computation. It should be noted that as far as the computational time is concerned the coupled MDS/LBM only consumes about 1/5 of that of MDS.

3.3 Flow and Heat Transfer in Micronozzle by Coupling of DSMC and FVM (Solid). Small satellites or microsatellites have developed very fast recently, and the micronozzle used to control satellites attitude and trajectory has become a research focus. Among different kinds of micronozzle, free molecular micro-electrothermal resist jet (FMMR) has attracted an increasing research attention (Fig. 10). When the low temperature propellant flows over the heating surface, the propellant molecules knock with it. The temperature of propellant raises. Then, the propellant rushes out of the nozzle with high speed and thrust is generated. The value of Kn of gas flow in micronozzle is basically in the transition flow ($0.1 < \mathrm{Kn} < 10.0$), thus DSMC is the most useful method to simulate the flow field. To simulate the flow and

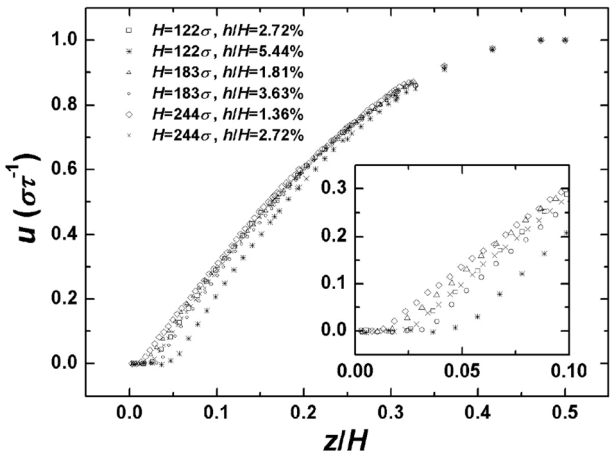

(a) Roughened channel (zero velocity at z=0)

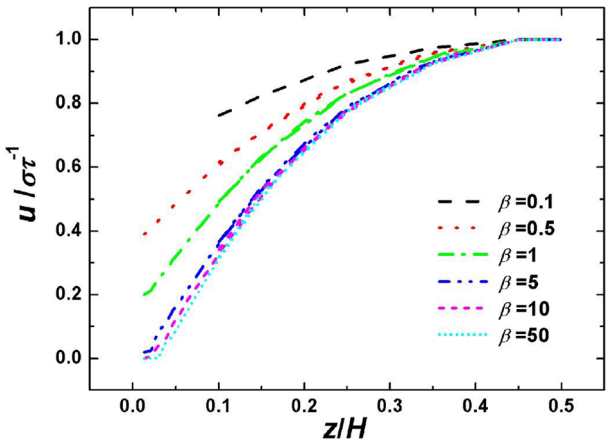

(b) Smooth channel (velocity slip at z=0)

Fig. 7 Comparison of velocity distribution for roughened and smooth channel

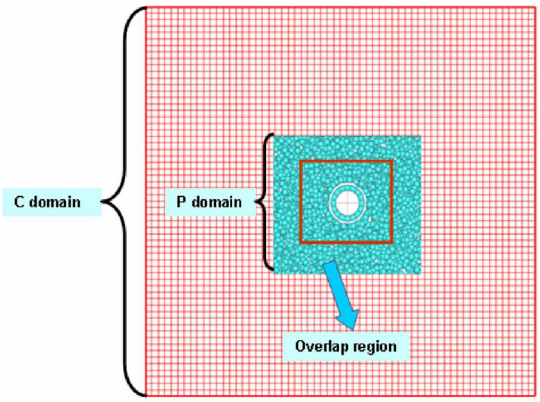

（a）Entire computational domain

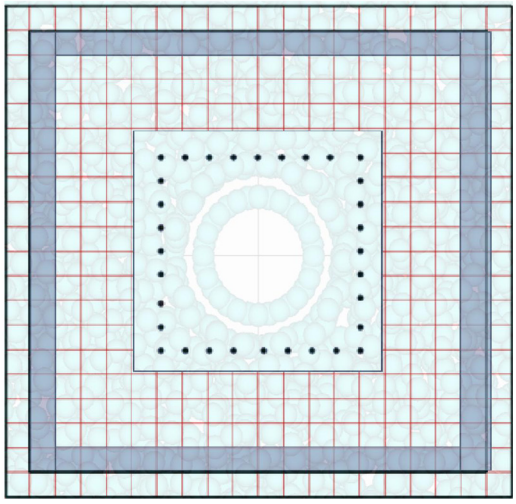

(b) Center part of the domain

Fig. 8 Flow past a nanotube simulated by coupled MD and LBM

Downloaded From: http://heattransfer.asmedigitalcollection.asme.org/ on 03/05/2013 Terms of Use: http://asme.org/terms

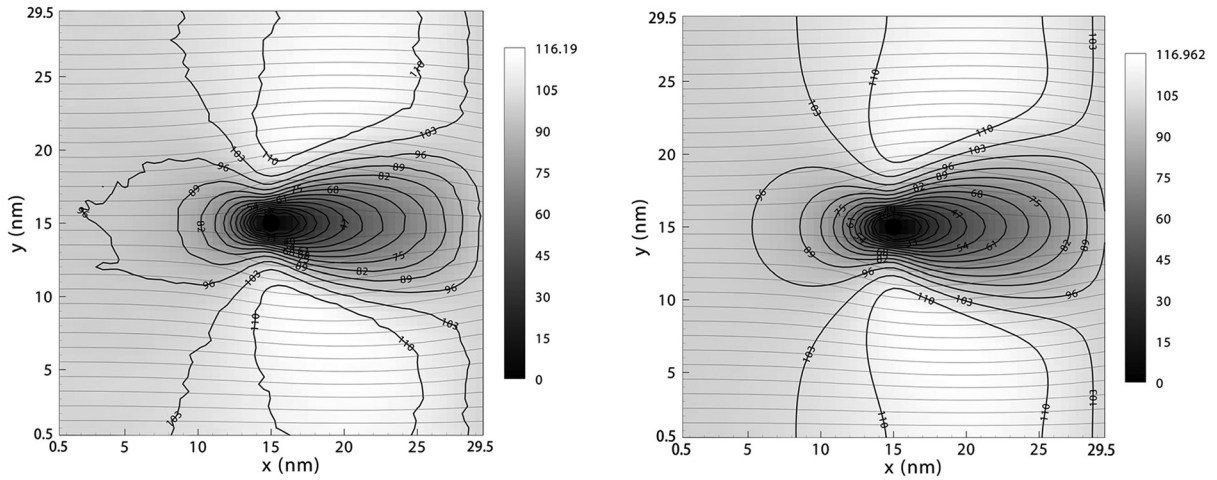

(a) Stream function form [76] by MDS

(b) Stream function form [81] by Coupled MDS and LBM

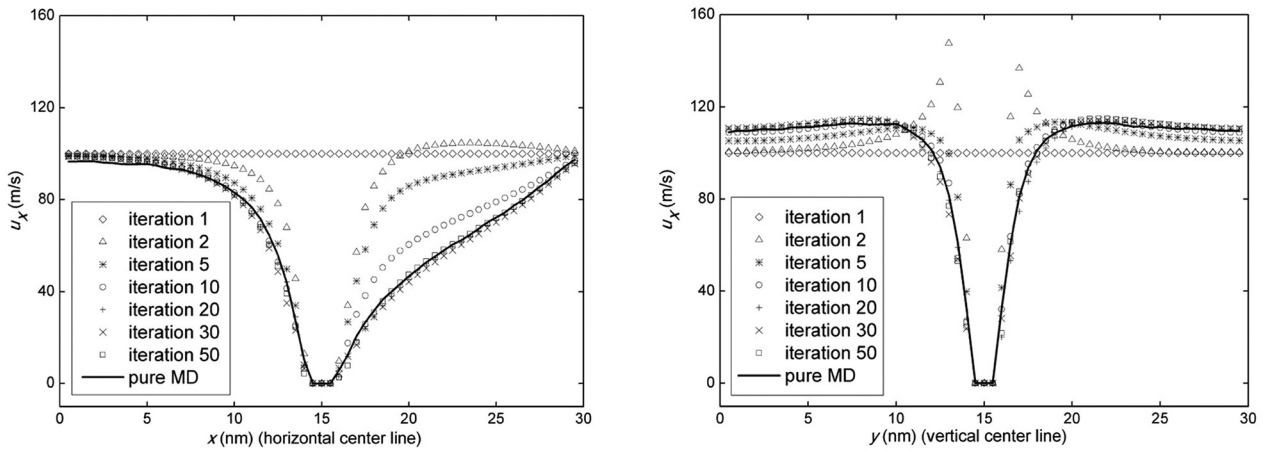

(c) u-velocity at horizontal center line

(d) u-velocity at vertical center line

Fig. 9 Results of flow past a nanotube by MDS and coupled MDS/LBM

heat transfer characteristics in the nozzle, DSMC-FVM coupled method was used [68]: in the flow regime DSMS was used while in the solid wall FVM was adopted. The Dirichlet–Neumann method was used to couple the temperature and heat flux at the boundary of flow field and solid area.

It can be imagined that the pressure in the flow field decreases gradually from the inlet to the outlet, which means that the number density of molecules decreases from inlet to outlet while the mean free path of molecules increases. Thus, the grid dimension along flow direction was gradually increased, so the number of molecules in each cell was approximately constant. The variable hard sphere model was used. Cercignani–Lampis–Lord model [14] was adopted to simulate the interaction between the solid surface, and the accommodation coefficient was 0.73.The inlet pressure, inlet temperature, and outlet pressure were set up before calculation. The statistical macroscopic velocity obtained from particle in the cells near the inlet boundary was used as the income velocity for new incoming particles. The propellant was argon. The temperature of heating surface was 600 K. The solid material was silicon with thermal conductivity of 149 W/m K.

Five cases were simulated with different inlet pressures. The inlet temperature was all set as 300 K. The major simulation results are shown in Table 1. It can be seen that the wall boundary temperature changes dramatically with the inlet pressure, so DSMC-FVM coupled simulation is necessary for FMMR. If temperature is set up before calculation, a large error may be caused.

3.4 Flow Around a Circular Cylinder by Coupling of FVM and LBM (CFVLBM) With Density Function Reconstruction Operator. The two-dimensional flow around a square/circular cylinder for low Reynolds numbers is studied in Refs. [82] and [83], respectively. The geometry and boundary conditions for flow around a circular cylinder are shown in Fig. 11. A uniform velocity $u_0 = (u_\infty, 0)$ is specified along the domain perimeter as physical boundary and zero velocities are imposed at the cylinder surface. The parameters are defined as follows: height $H = 1.8$, cylinder radius $r = 0.005$, density $\rho = 1.0$, velocity $u_\infty = 0.01$, grid length $\Delta x = \Delta y = 2 \times 10^{-4}$. The Reynolds number is defined by $\mathrm{Re} = 2u_\infty r/\nu$.

For flow around a circular cylinder there are three characteristic parameters: the length of the recirculation region L, the separation angle θ, and the drag coefficient C_D. C_D is defined as

$$C_D = \frac{1}{\rho u_\infty^2 r} \int S \cdot n dl \tag{9}$$

where n is the normal direction of the cylinder wall and S is the stress tensor

$$S = -pI + \rho\nu(\nabla u + u\nabla) \tag{10}$$

Downloaded From: http://heattransfer.asmedigitalcollection.asme.org/ on 03/05/2013 Terms of Use: http://asme.org/terms

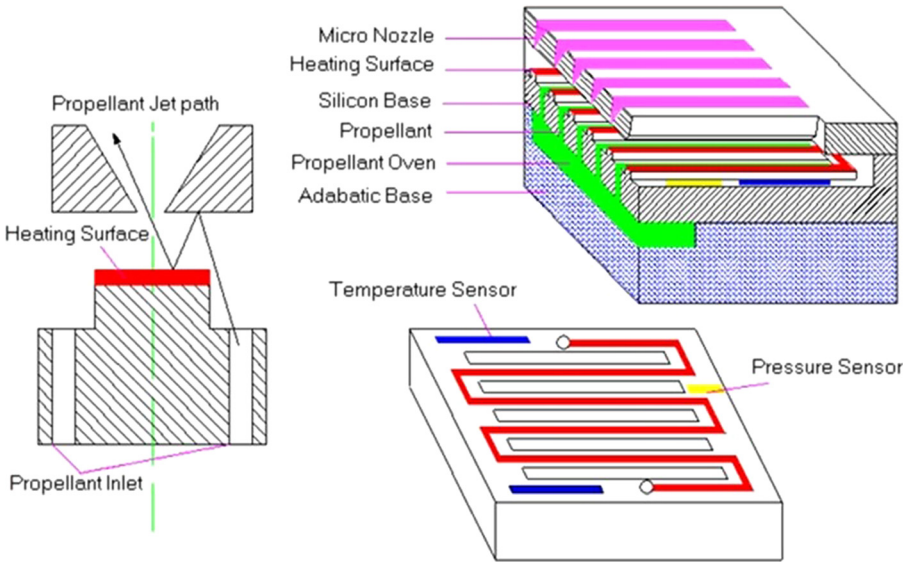

Fig. 10 Schematic diagram of FMMR

The predicted drag coefficient C_D and the geometry parameter L and θ are listed in Table 2. All the parameters predicted by CFVLBM agree well with the results of previous studies for each Re.

3.5 Fluid Flow Around/Through a Porous Media Square Cylinder Simulated by Coupled LBM/FVM. In Ref. [42], the flow around and through a porous media square cylinder is simulated by CFVLBM, fully showing the role of LBM in displaying the flow details in complicated configuration. Flow simulation results by CFVLBM is presented in Figs. 12(*a*) and 12(*b*). It would be very difficult (if not impossible) for FVM to obtain such fine flow resolution. To compare the computational time for flow around a solid square cylinder, three numerical methods have been used: LBM, multiblock LBM, and CFVLBM. Figure 12(*c*) shows the three-block structure used in the simulation. In the multiblock LBM, the grid system in the center black region is the finest where the porous media cylinder locates and that of the outside region is the coarsest. Comparison of the computational time is shown in Fig. 13. It can be seen that among three methods adopted the CFVLBM can have three orders faster than that of multiblock LBM, not mentioned to the single block LBM. It should be noted that in this comparison, the cylinder is a sold one without complicated structure in it. This is because for FVM, it is very difficult to simulate a complicated structure as the cylinder shown in Fig. 12(*a*). Thus, only the solid cylinder is used for comparison purpose.

3.6 Natural Convection in a Square Cavity by Coupling of Temperature and Temperature Distribution Function. Natural convection in a square cavity is one of the benchmark problems in computational heat transfer. This problem is taken to verify the feasibility of the reconstruction operator of the temperature density function. The domain is vertically divided into three regions: the left part is simulated FVM, the right part by LBM, and center part is the hand-shaking area. Simulation was conducted for $\mathrm{Ra} = 10^3$, 10^4, 10^5, and 10^6. In the computations, the density distribution function and the temperature distribution function in the coupling region were determined according to the reconstruction operators Eqs. (6) and (7), respectively. Partial simulation results are presented in Figs. 14 and 15 for temperature contours and vorticity contours, respectively. In these figures results from FLUENT, self-coded FVM, LBM, and CFVLBM are compared. It can be seen that the simulation results by CFVLBM agree with others quite well. It is worth noting that according to authors' experience in the hand-shaking region the smoothness of vorticity contours is the most difficult to obtain and that of stream lines is the easiest to get, because vorticity is the first derivative of velocity, while streamlines are the integration of velocity. It can be seen from Fig. 15 that for the case studied the vorticity contour smoothness is quite good.

4 Further Research Needs

As indicated above, the idea of multiscale simulation has been widely adopted in the material science for about 10 years and great achievements have been attained. A typical successful example in the material science can be found from Ref. [24]. In Ref. [24], the study of a crack performance in the silicon material is conducted by the multiscale simulation: the tight binding (TB, which is a microlevel simulation method from quantum mechanics) is used to simulate the crack tip, at the interface between crack and continuum material, coupling between TB and MDS is conducted. Then, MDS is adopted to simulate the behavior of the region around the crack. At the interface where MDS meets FEM information is transferred between the two methods.

For the heat/mass transfer processes in the PEMFC, a full multiscale simulation may be conducted as shown in Fig. 16. This ideal multiscale simulation may be called full multiscale

Table 1 Major simulation results of example 3

Inletpressure (Pa)	Throat pressure (Pa)	Throat Knudsen number	Throat velocity (m/s)	Throat Mach number	Throat Reynolds number	Solid 1 Temperature (K)	Flow rate(kg/s)	Thrust (N)	Specific impulse (S)
500	218	0.52	218	0.51	1.2	567	2.22×10^{-05}	0.013	58
1000	459	0.25	237	0.56	2.8	561	5.09×10^{-05}	0.030	59
2000	974	0.11	257	0.62	7.1	529	1.23×10^{-04}	0.073	61
5000	2802	0.031	262	0.68	27.6	433	4.18×10^{-04}	0.25	61
10,000	6572	0.012	262	0.71	72.5	423	1.01×10^{-03}	0.63	63

Downloaded From: http://heattransfer.asmedigitalcollection.asme.org/ on 03/05/2013 Terms of Use: http://asme.org/terms

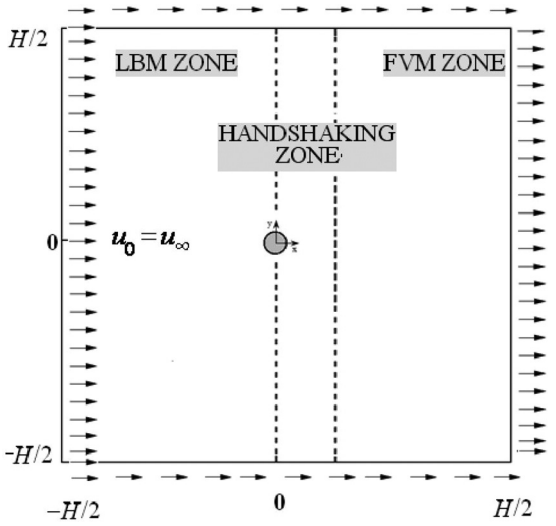

Fig. 11 Flow around a circular cylinder

simulation. From the above presentation, we may be clearly aware of the fact that we have a long way to go in order to implement such a full multiscale simulation for complicated heat/mass transfer process such as one in PEMFC. Taking the simulation of catalyst layer and membrane layer by MDS as an example, the present day computer capability for MD simulation is in the order of tens of nanometers, while the two thicknesses are tens of micrometers and several hundreds of micrometers, respectively. In addition, the very complicated molecular structure of the membrane provides many difficulties to the transport process simulation by MDS.

Attention is now turned to another important example: the phase change heat transfer of refrigerants. As indicated above up to now we are still unable to numerically predict the performance of enhanced surface structure such as Thermoexcel. In the authors' opinion, here is an another example that multiscale simulation can play a role: MDS is used for condensation of vapor on a complicated surface structure, LBM is adopted for the liquid flow in the condensed film and FVM for the temperature distribution in the solid. In order that the effects of surface structure shape and geometric factors can be sensed by the condensed film, its thickness should be at least more than one micrometer and its surface area at least in tens of millimeters. These dimensions are far out of the present day computer capability for MDS. In addition for the atomistic scales, the development of accurate potentials between dissimilar materials (elements and phases) is critical for heat and mass transfer, and up to now we do not have satisfied potential functions for both complex fluids such as water and refrigerants and for the combination of such fluids with engineering metals as copper and iron.

The third issue is about numerical uncertainty analysis for the results of multiscale simulation. Most methods developed so far

Table 2 Comparisons of simulation results of example 4

Re	Authors	Method	C_D	L/r	θ (deg)
10	Dennis and Chang [84]	N.S.	2.846	0.53	29.6
	He and Doolen [85]	ISLBM	3.170	0.474	26.89
	Guo and Zhao [86]	FDLBM	3.049	0.486	28.13
	Imamura et al. [87]	GILBM	2.848	0.478	26.0
	Present work	CFVLBM	2.810	0.51	29.2
20	Dennis and Chang [84]	N.S.	2.045	1.88	43.7
	He and Doolen [85]	ISLBM	2.152	1.842	42.96
	Guo and Zhao [86]	FDLBM	2.048	1.824	43.59
	Imamura et al. [87]	GILBM	2.051	1.852	43.3
	Present work	CFVLBM	2.010	1.85	43.2
40	Dennis and Chang [84]	N.S.	1.522	4.69	53.8
	He and Doolen [85]	ISLBM	1.499	4.49	52.84
	Guo and Zhao [86]	FDLBM	1.475	4.168	53.44
	Imamura et al. [87]	GILBM	1.538	4.454	52.4
	Present work	CFVLBM	1.511	4.44	53.5

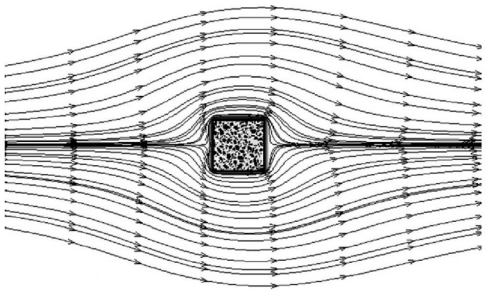

(a) Flow field around and through porous square cylinder

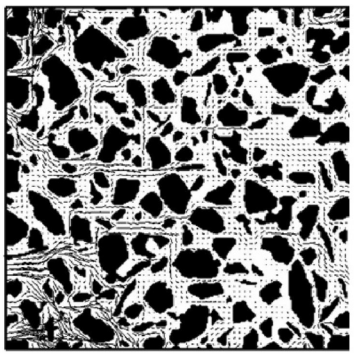

(b) Flow details in porous square cylinder

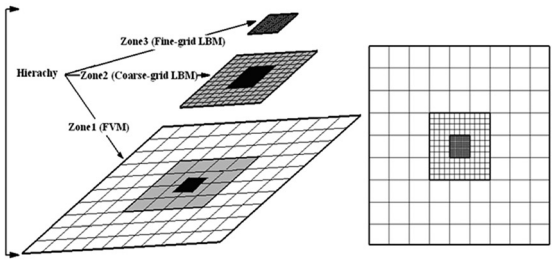

(c) Computational domain

Fig. 12 Flow around/through a porous square cylinder

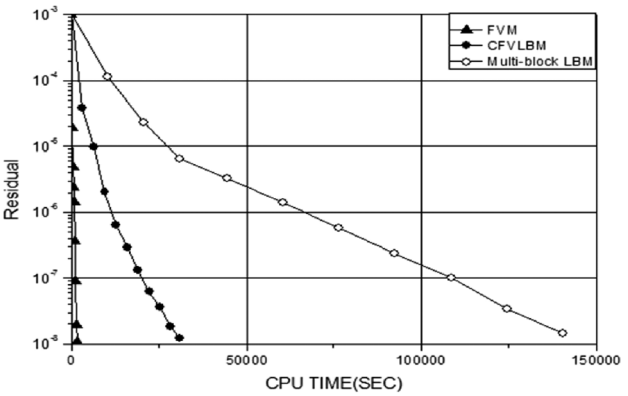

Fig. 13 Comparison of computational times for flow around a solid cylinder

Downloaded From: http://heattransfer.asmedigitalcollection.asme.org/ on 03/05/2013 Terms of Use: http://asme.org/terms

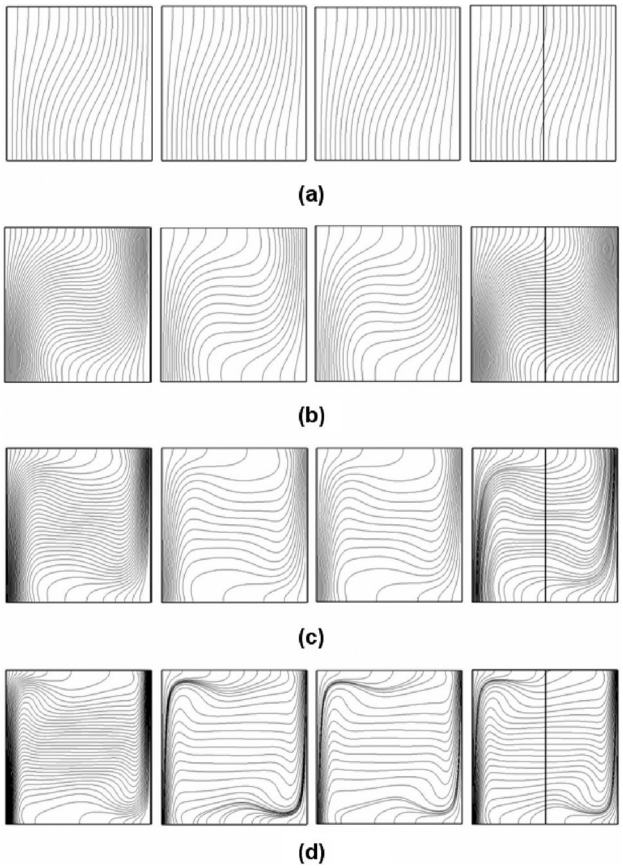

Fig. 14 The isotherm: (a) $Ra = 10^3$, (b) $Ra = 10^4$, (*c*) $Ra = 10^5$, and (*d*) $Ra = 10^6$ (the results of FLUENT, FVM, LBM, and CFVLBM are shown from left to right)

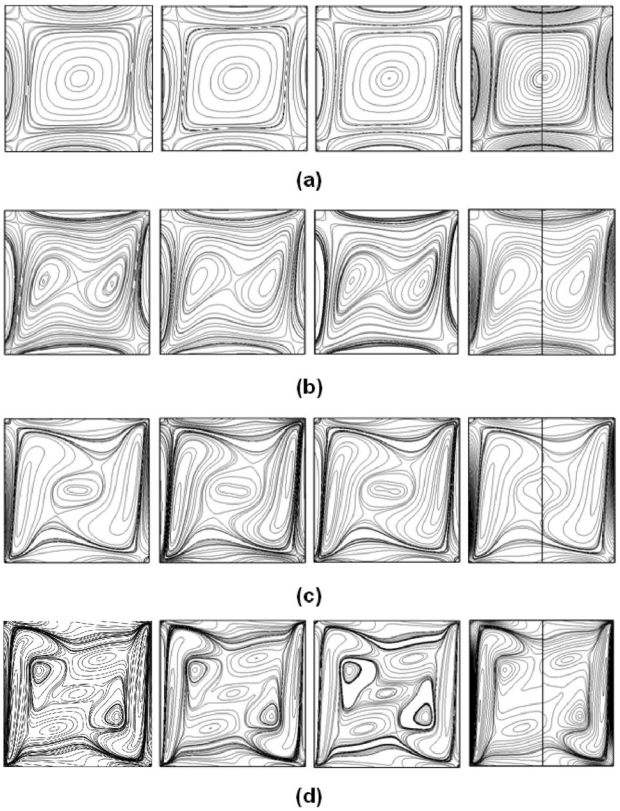

Fig. 15 The contour lines of vorticity (a) Ra = 103, (b) Ra = 104, (*c*) Ra = 105, and (*d*) Ra = 106 (the results of FLUENT, FVM, LBM, and CFVLBM are shown from left to right)

are mainly for the macroscopic methods [88,89]. For the DSMC [91] presented some analysis method and [92,93] made statistical error analysis for both DSMC and MDS. Few papers presented methods for analyzing numerical uncertainty of results from multiscale simulation. Reference [90] is titled with "multiscale simulation;" however, "multiscale" in that paper is really means grids with large variation of size. The governing equations for the different grids are the same. Thus, this is not the multiscale simulation specified in the present paper.

From the two examples (transport process in PEMFC and refrigerant condensation) and the above discussion, we may propose following further research needs for the multiscale simulations:

(1) improve greatly the computational efficiencies of mesoscale and microscale numerical approaches;
(2) develop appropriate potential functions for fluids with complex molecule structures (water and refrigerants);
(3) innovate more efficient coupling techniques (operators) for MDS-FVM, DSMC-FVM with high efficiency and stability;
(4) establish uncertainty analysis approach for the numerical results of multiscale simulations.

5 Conclusions

Most phenomena and processes in science and engineering are multiscale in nature. With the rapid development in science and technology the importance of study from multiscale view point becomes more and more obvious. In heat transfer field, multiscale problems may be classified as multiscale process and multiscale system. For the multiscale process, the method of "solving regionally and coupling at the interfaces" is the most promising one. In such method, the key issue is the exchange information at the interfaces. The exchange of information should be conducted in a way that is physically meaningful, mathematically stable, computationally efficient, and easy to be implemented. The key point is the establishment of the reconstruction operator, which transforms the data of few variables of macroscopic computation to a large amount of variables of microscale or mesoscale simulation. For different coupling cases, the existing methods for such operators are briefly reviewed. Six examples of multiscale simulation of heat transfer and fluid flow problems are presented. It is found that for multiscale process, the method of solving regionally and coupling at the interfaces can get converged solution faster by several orders than the uniform mesoscale or microscale numerical method for the entire domain.

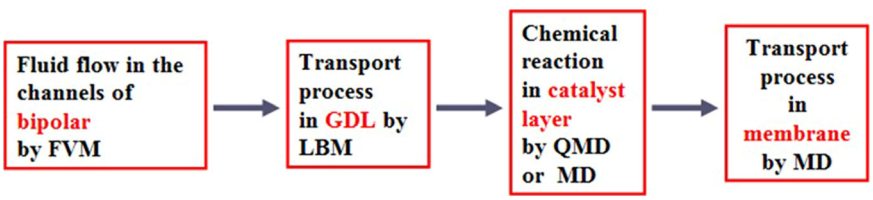

Fig. 16 Schematic diagram for a full multiscale simulation of PEMFC

Downloaded From: http://heattransfer.asmedigitalcollection.asme.org/ on 03/05/2013 Terms of Use: http://asme.org/terms

The numerical study for the multiscale process of heat transfer and fluid flow problems is still in its childhood and its engineering application is in its infancy. Further, researches are highly required to establish robust and quick-convergent numerical solution approaches.

Acknowledgment

The authors' papers cited in this paper are the research results of the key projects supported by the National Natural Science Foundation of China (51136004,50736005). Thanks also go to our students (Dr. J. Sun, Dr. H. Xu, Dr. H.B. Luan, Dr. Z.X. Sun, Dr. W.J. Zhou, and Mr. Z. Tang) for their helps in the preparation of some figures.

Nomenclature

a_T = thermal diffusivity
C_D = compression operator (Dirichlet type)
C_D = drag coefficient
C_N = compression operator (Neumann type)
c_s = lattice speed of sound
f_i = density distribution function
f_i^{eq} = equilibrium density distribution function
F_i = temperature distribution function
F_i^{eq} = equilibrium temperature distribution function
H = height
I = unit tenser
k_b = Boltzmann constant
Kn = Knudsen number
l, L = length
M = mass of continuum fluid element
N_j = total molecule number in jth bin
p = pressure
p_n = momentum of nth molecule
q = flux
Q = specific flow property
r = radius
r_c = cutoff radius
Ra = Rayleigh number
R_D = reconstruction operator (Dirichlet type)
$\mathcal{S}, \mathcal{S}$ = stress tensor
T = temperature
u = microscopic (mesoscopic) parameter
u= velocity vector (in Eq. (10))
u_∞= far field velocity
U = macroscopic parameter

Greek Symbols

α,β = coordinates in LBM
δt, Δt = time step
Δx, Δz = length step
∇ = gradient
ε = energy characteristic parameter in L-J function
φ= potential function
λ = thermal conductivity
ν = kinematic viscosity
θ = separation angle
ρ = density
σ = characteristic length in L-J potential function
τ = relaxation factor of density distribution function
τ' = relaxation factor of temperature distribution function
ω_i = weighting factor
∂_{x_α} = partial derivative with respect to x_α

References

[1] Weinan, E., and Engquist, B., 2003, "Multiscale Modeling and Computation," Not. Am. Math. Soc., **50**(9), pp. 1062–1070.
[2] Zhang, Z. M., 2007, *Nano/Microscale Heat Transfer* McGraw-Hill, New York, p. 2.
[3] Patankar, S. V., 1980, *Numerical Heat Transfer and Fluid Flow*, McGraw-Hill, New York.
[4] Versteeg, H. K., and Malalsekera, W., 1955, *An Introduction to Computational Fluid Dynamics. The Finite Volume Method*, Longmann Scientific and Technical, Essex.
[5] Shyy, W., Thakur, S. S., Ouyang, H., Liu, J., and Blosch, E., 1997, *Computational Techniques for Complex Transport Phenomena*, Cambridge University Press, Cambridge.
[6] Tao, W. Q., 2001, *Numerical Heat Transfer*, 2nd ed., Xi'an Jiaotong University Press, Xi'an.
[7] Blazek, J., 2001, *Computational Fluid Dynamics: Principles and Applications*, Elsevier, Amsterdam.
[8] Jaluria, Y., and Torrance, K. E., 2003, *Computational Heat Transfer*, 2nd ed., Taylor & Francis, New York.
[9] Qian, Y. H., Humiere, D. D., and Lallemand, P., 1992, "Lattice BGK Models for Navier-Stokes Equation," Europhys. Lett., **17**(6), pp. 479–485.
[10] Chen, S., and Doolen, G. D., 1998, "Lattice Boltzmann Method for Fluid Flows," Annu. Rev. Fluid Mech., **30**, pp. 329–364.
[11] Wof-Gladrow, D. A., 2000, *Lattice-Gas Cellular Automatta and Lattice Boltzmann Models, An Introduction*, Springer, Berlin.
[12] Succi, S., 2001, *The Lattice Boltzmann Equation for Fluid Dynamics and Beyond*, Clarendon Press, Oxford.
[13] He, Y. L., Wang, Y., and Li, Q., 2009, *Lattice Boltzmann Method: Theory and Applications*, Science Press, Beijing.
[14] Bird, G. A., 1994, *Molecular Gas Dynamics and the Direct Simulation of Gas Flows*, Clarendon Press, Oxford.
[15] Fan, J., and Shen, C., 2001, "Statistical Simulation of Low-Speed Rarefied Gas Flows," J. Comput. Phys., **167**, pp. 393–412.
[16] Shu, C., Mao, X. H., and Chew, Y. T., 2005, "Particle Number per Cell and Scaling Factor Effect on Accuracy of DSMC Simulation of Micro Flows," Int. J. Numer. Methods Heat Fluid Flow, **15**(8), pp. 827–841.
[17] Sun, Z. X., Tang, Z., He, Y. L., and Tao, W. Q., 2011, "Proper Cell Dimension and Number of Particles per Cell for DSMC," Comput. Fluids (to be published).
[18] Allen, M. P., and Tildesley, D. J., 1987, *Computer Simulation of Liquids*, Clarendon Press, Oxford.
[19] Haile, J. M., 1992, *Molecular Dynamics Simulation-Elementary Methods*, Wiley-Interscience/John Wiley & Sons Inc., New York.
[20] Rapaport, D. C., 1995, *The Art of Molecular Dynamics Simulation*, Cambridge University Press, Cambridge.
[21] O'Connel, S. T., and Thompson, P. A., 1995, "Molecular Dynamics-Continuum Hybrid Computations: A Tool for Studying Complex Fluid Flows," Phys. Rev. E, **52**(6), pp. R5792–R5795.
[22] Luan, H. B., 2011, "Coupling of Mesoscopic Lattice Boltzmann Method and Macro/Microscopic Method for Simulating Multiscale Thermal and Fluid Science Problems," Ph.D. dissertation, School of Energy and Power Engineering, Xi'an Jiaotong University, Xi'an.
[23] Broughton, J. Q., Abraham, F. F., Bernstein, N., and Kaxiras, E., 1999, "Concurrent Coupling of Length Scales: Methodology and Application," Phys. Rev. B, **60**(4), pp. 2391–2403.
[24] Abraham, F. F., 2000, "Dynamically Spanning the Length Scales From the Quantum to the Continuum," Int. J. Mod. Phys. C, **11**(6), pp. 1135–1148.
[25] Wagner, G. J., and Liu, W. K., 2002, "Coupling of Atomistic and Continuum Simulations Using a Bridging Scale Decomposition," J. Comput. Phys., **190**, pp. 249–274.
[26] Tao, W. Q., and He, Y. L., 2009, "Recent Advances in Multiscale Simulation of Heat Transfer and Fluid Flow Problems," Prog. Comput. Fluid Dyn., **9**(3/4/5), pp. 151–157.
[27] Moin, P., and Mahesh, K., 1998, "Direct Numerical Simulation: A Tool in Turbulence Research," Annu. Rev. Fluid Mech., **30**, pp. 39–78.
[28] Tsien, H.-S., 1946, "Superaerodynamics, the Mechanics of Rarified Gas," J. Aeronaut. Sci., **13**, pp. 653–664.
[29] Devienne, F. M., 1965, "Low Density Heat Transfer," *Advances in Heat Transfer*, Vol. **2**, J. P. Hartnett and T. F. Irvine, Jr., eds., Academic Press, New York, pp. 271–356.
[30] Eikerling, M., and Kornyshev, A. A., 1998, "Modeling the Performances of Cathode Catalyst Layers of Polymer Electrolyte Fuel Cells," J. Electroanal. Chem., **453**, pp. 89–106.
[31] Ticianelli, E. A., Derouin, C. R., Redondo, A., and Srinivasan, S., 1988, "Methods to Advance Technology of Proton Exchange Membrane Fuel Cells," J. Electrochem. Soc., **135**(9), pp. 2209–2214.
[32] Ticianelli, E. A., Derouin, C. R., and Srinivasan, S., 1988, "Localization of Platinum in Low Catalyst Loading Electrodes to Attain High Power Densities in SPE Fuel Cells," J. Electroanal. Chem., **251**, pp. 275–295.
[33] Tao, W. Q., Min, C. H., He, Y. L., Liu, X. L., Yin, B. H., and Jiang, W., 2006, "Parameter Sensitivity Examination and Discussion of PEM Fuel Cell Simulation Model Validation, Part I: Current Status of Modeling Research and Model Development," J. Power Source, **160**, pp. 359–373.
[34] Min, C. H., He, Y. L., Liu, X. L., Yin, B. H., Jiang, W., and Tao, W. Q., 2006, "Parameter Sensitivity Examination and Discussion of PEM Fuel Cell Simulation Model Validation, Part II: Results of Sensitivity Analysis and Validation of the Model," J. Power Source, **160**, pp. 374–385.
[35] Nakayama, W., Daikoku, T., Kuwahara, H., and Kakizaki, K., 1975, "High-Flux Heat Transfer Surface 'Thermoexcel," Hitachi Rev., **24**(8), pp. 329–334.
[36] Tang, L., and Joshi, Y., 1999, "Integrated Thermal Analysis of Natural Convection Air Cooled Electronic Enclosure," ASME J. Electron. Packag., **121**, pp. 108–115.

Downloaded From: http://heattransfer.asmedigitalcollection.asme.org/ on 03/05/2013 Terms of Use: http://asme.org/terms

[37] Nie, Q., and Joshi, Y., 2008, "Multiscale Thermal Modeling Methodology for Thermoelectrically Cooled Electronic Cabinets," Numer. Heat Transfer, Part A, **53**(3), pp. 225–248.
[38] Tang, L., and Joshi, Y. K., 2005, "A Multi-Grid Based Multi-Scale Thermal Analysis Approach for Combined Mixed Convection, Conduction, and Radiation Due to Discrete Heating," ASME J. Heat Transfer, **127**(1), pp. 18–26.
[39] Weinan, E., and Engquist, B., 2003, "The Heterogeneous Multiscale Methods," Commun. Math. Sci., **1**(1), pp. 87–133.
[40] Weinan, E., Engquist, B., Li, X., Ren, W., and Vanden-Eijnden, E., 2007, "The Heterogeneous Multiscale Methods: A Review," Commun. Comput. Phys., **2**(3), pp. 367–450.
[41] Li, Z. H., and Zhang, H. X., 2004, "Study on Gas Kinetic Unified Algorithm for Flows from Rarefied, Transition to Continuum," J. Comput. Physics, **193**(2), pp. 708–738.
[42] Luan, H. B., Xu, H., Chen, L., Sun, D. L., and Tao, W. Q., 2011, "Evaluation of the Coupling Finite Volume Method and Lattice Boltzmann Method for Fluid Flows Around Complex Geometries," Int. J. Heat Mass Transfer, **54**, pp. 1975–1985.
[43] Lu, T., Shih, T. M., and Liem, C. B., 1997, *Domain Decomposition Methods — New Numerical Techniques for Solving PDE*, Science Press, Beijing.
[44] Schwarz, H. A., 1890, "Gesammelete Mathematische Abhandlungen," *Vierteljahrsschrift der Naturforschenden Geselschaft in Zurich*, Vol. **2**, Springer, Berlin, pp. 272–286.
[45] Wagner, G., Flekkøy, E., Feder, J., and Jøssang, T., 2002, "Coupling Molecular Dynamics and Continuum Dynamics," Comput. Phys. Commun., **147**, pp. 670–673.
[46] Nie, X. B., Chen, S. Y., and Robbins, M. O., 2004, "Hybrid Continuum-Atomistic Simulation of Singular Corner Flow," Phys. Fluids, **16**, pp. 3579–3591.
[47] Werder, T., Walther, J. H., and Koumoutsakos, P., 2005, "Hybrid Atomistic-Continuum Method for the Simulation of Dense Fluid Flows," J. Comput. Phys., **205**, pp. 373–390.
[48] Liu, J., Chen, S. Y., Nie, X. B., and Robbins, M. O., 2007, "A Continuum Atomistic Simulation of Heat Transfer in Micro- and Nano-Flow," J. Comput. Phys., **227**, pp. 279–291.
[49] Wang, Y. C., and He, G. W., 2007, "A Dynamic Coupling Model for Hybrid Atomistic-Continuum Computations," Chem. Eng. Sci., **62**, pp. 3574–3579.
[50] Yen, T. H., Soong, C. Y., and Tzeng, P. H., 2007, "Hybrid Molecular Dynamics-Continuum Simulation for Nano/Mesoscale Channel," Microfluid. Nanofluid., **3**, pp. 665–675.
[51] Yasuda, S., and Yamamoto, R., 2008, "A Model for Hybrid Simulation of Molecular Dynamics and Computational Fluid Dynamics," Phys. Fluids, **20**, 113101.
[52] Sun, J., He, Y. L., and Tao, W. Q., 2009, "Molecular Dynamics and Continuum Hybrid Simulation for Condensation of Gas Flow in a Micorchannel," Microfluid. Nanofluid., **7**(3), pp. 407–422.
[53] Sun, J., He, Y. L., and Tao, W. Q., 2009, "Scale Effect on Flow and Thermal Boundaries in Micro/Nano-Channel Flow Using Molecular-Continuum Hybrid Simulation Method," Int. J. Numer. Methods Eng., **81**(2), pp. 207–228.
[54] Hash, B., and Hassan, A., 1997, "Two-Dimensional Coupling Issues of Hybrid DSMC/Navier-Stokes Solvers," AIAA Paper No. 1997-2507.
[55] Wu, J.-S., Lian, Y.-Y., Cheng, G., Koomullil, P. R., and Tseng, K.-C., 2006, "Development and Verification of a Coupled DSMC-NS Scheme Using Unstructured Mesh," J. Comput. Phys., **219**, pp. 579–607.
[56] Roveda, R., Goldstein, D. B., and Varghese, P. L., 1998, "Hybrid Euler/Particle Approach for Continuum/Rarefied Flows," J. Spacecr. Rockets, **35**, pp. 258–265.
[57] Aktas, O., and Aluru, L. R., 2002, "A Combined. Continuum/DSMC Technique for Multiscale Analysis of Microfluidic Filters," J. Comput. Phys., **178**, pp. 342–372.
[58] Wu, J. S., Lian, Y. Y., Cheng, G., and Chen, Y. S., 2007, "Parallel Hybrid Particle-Continuum (DSMC-NS) Flow Simulation Using 3-D Unstructured Mesh," *Parallel Computational Fluid Dynamics-Parallel Computing and its Applications*, J. H. Kwon, A. Ecer, J. Periaux, N. Satofuka, and P. Fox, eds., Elsevier, Amsterdam, pp. 1–10.
[59] Schwartzentruber, T. E., Scalabrin, L. C., and Boyd, I. D., 2006, "Hybrid Particle-Continuum Simulations of Non-Equilibrium Hypersonic Blunt Body Flow Fields," AIAA Paper No. 2006-3602.
[60] Wijesinghe, H. S., Hornung, R. D., Garcia, A. L., and Hadjicons-tantinou, N. G., 2004, "Three-Dimensional Hybrid Continuum-Atomistic Simulations for Multiscale Hydrodynamics," ASME J. Fluids Eng., **126**(3), pp. 769–777.
[61] Wong, J., Ketsdever, A., and Reed, H., 2003, "Numerical Modeling of the Free Molecule Micro-Resistojet Prototype and Next Generation Designs Evaluation," AIAA Paper No. 2003-3581.
[62] Ahmed, Z., Gimelshein, S., and Ketsdever, A., 2005, "Numerical Analysis of Free Molecule Micro-Resistojet Performance," AIAA Paper No. 2005-4262.
[63] Gimelshein, S., Markelov, G., Lilly, T., Selden, N., and Ketsdever, A., 2005, "Experimental and Numerical Modeling of Rarefied Gas Flows Through Orifices and Short Tubes," *24th International Symposium on Rarefied Gas Dynamics*, pp. 437–443.
[64] Liu, M., Zhang, X., Zhang, G., and Chen, Y., 2006, "Study on Micronozzle Flow and Propulsion Performance Using DSMC and Continuum Methods," Acta Mech. Sinica, **22**, pp. 409–416.
[65] Xie, C., 2007, "Characteristics of Micronozzle Gas Flows," Phys. Fluids, **19**, 037102.
[66] Alexeenko, A., Levin, D., Fedosov, D., and Gimelshein, G., 2005, "Performance Analysis of Microthrusters Based on Coupled Thermal-Fluid Modeling and Simulation," J. Propul. Power, **21**(1), pp. 95–101.
[67] Alexeenko, A., Fedosov, D., Gimelshein, S., Levin, D., and Collins, R., 2006, "Transient Heat Transfer and Gas Flow in a MEMS-Based Thruster," J. Microelectromech. Syst., **15**(1), pp. 181–194.
[68] Sun, Z. X., Li, Z. Y., He, Y. L., and Tao, W. Q., 2009, "Coupled Solid (FVM)-Fluid (DSMC) Simulation of Micro-Nozzle With Unstructured-Grid," Microfluid. Nanofluid., **7**, pp. 621–631.
[69] Succi, S., Filippova, O., Smith, G., and Kaxiras, E., 2001, "Applying the Lattice Boltzmann Equation to Multi-Scale Fluid Problems," Comput. Sci. Eng., **3**(6), pp. 26–37.
[70] Albuquerque, P., Alemani, D., Chopard, B., and Leone, P., 2004, "Coupling a Lattice Boltzmann and a Finite Difference Scheme," *International Conference on Computational Science—ICCS 2004 (Lecture Notes in Computer Science)*, M. Bubak, G. D. van Albada, P. M. Sloot, and J. Dongarra, eds., Springer, Berlin, Vol., **3039**, pp. 540–547.
[71] Van Leemput, P., Samaey, G., Lust, K., Roose, D., and Kevrekidis, I. G., 2006, "Numerical and Analytical Spatial Coupling of a Lattice Boltzmann Model and a Partial Differential Equation," *Model Reduction and Coarse-Graining Approaches for Multiscale Phenomena*, A. N. Gorban, N. Kazantzis, I. G. Kevrekidis, H. C. Ottinger, and C. Theodoropoulos, eds., Springer, Berlin, pp. 423–441.
[72] Xu, H., 2009, "Lattice Boltzmann Model for Turbulent Fluid Flow Simulations and its Application in Multiscale Analysis," Ph.D. dissertation, Xi'an Jiaotong University, Xi'an.
[73] Xu, H., Luan, H. B., and Tao, W. Q., 2011, "A Correction Lifting Relation of Macroscopic Variables and Microscopic Variables in Lattice Boltzmann Method," (submitted).
[74] Luan, H. B, Xu, H., Chen, L., and Tao, W. Q., 2010, Coupling Between FVM and LBM for Heat Transfer and Fluid Flow, Chin. Sci. Bull., **55**(32), pp. 3128–3140.
[75] Horbach, J., and Succi, S., 2006, "Lattice Boltzmann Versus Molecular Dynamics Simulation of Nanoscale Hydrodynamic Flows," Phys. Rev. Lett., **96**, 224503.
[76] Dupuis, A., Kotsalis, E. M., and Koumoutsakos, P., 2007, Coupling Lattice Boltzmann and Molecular Dynamics Models for Dense Fluids, Phys. Rev. E, **75**, 046704.
[77] Dzmitry, H., Drona, K., and Ulrich, T., 2004, "Coupled Lattice-Boltzmann and Finite-Difference Simulation of Electroosmosis in Microfluidic Channels," Int. J. Numer. Methods Fluids, **46**, pp. 507–532.
[78] Sun, J., He, Y. L., Tao, W. Q., Yin, X., and Wang, H. S., 2009, "Roughness Effect on Flow and Thermal Boundaries in Microchannel/nanochannel Flow Using Molecular Dynamics-Continuum Hybrid Simulation," Int. J. for Numer. Methods in Engineering.
[79] Stoddard, S. D., and Ford, J., 1973, "Numerical Experiment on the Stochastic Behavior of a Lennard-Jones Gas System," Phys. Rev. A, **8**(3), pp. 1504–1512.
[80] Dupuis, A., and Koumoutsakos, P., 2007, "Effects of Atomistic Domain Size on Hybrid Lattice Boltzmann-Molecular Dynamics Simulations for Dense Fluids," Int. J. Mod. Phys. C, **18**(4), pp. 844–651.
[81] Zhou, W. J., Luan, H. B., Sun, J., He, Y. L., and Tao, W. Q., "A Molecular Dynamics and Lattice Boltzmann Hybrid Method for Dense Fluid Flow," Int. J. Heat Mass Transfer (submitted).
[82] Hadjiconstantinou, N. G., and Patera, A. T., 1997, "Heterogeneous Atomistic-Continuum Representations for Dense Fluid Systems," Int. J. Mod. Phys. C, **8**(4), pp. 967–976.
[83] Luan, H. B., Xu, H., Chen, L., Sun, D. L., and Tao, W. Q., 2010, "Numerical Illustrations of the Coupling Between Lattice Boltzmann Method and Finite-Type Macro-Numerical Methods," Numer. Heat Transfer, B, **57**(2), pp. 147–170.
[84] Dennis, S., and Chang, G., 1970, "Numerical Solutions for Steady Flow Past a Circular Cylinder at Reynolds Number up to 100," J. Fluid Mech., **42**, pp. 471–489.
[85] He, X., and Doolen, G., 1997, "Lattice Boltzmann Method on Curvilinear System: Flow Around a Circular Cylinder," J. Comput. Phys., **134**, pp. 306–315.
[86] Guo, Z., and Zhao, T., 2003, "Explicit Finite-Difference Lattice Boltzmann Method for Curvilinear Coordinates," Phys. Rev. E, **67**, 066709.
[87] Imamura, T., Suzuki, K., Nakamura, T., and Yoshida, M., 2005, "Acceleration of Steady State Lattice Boltzmann Simulation on Non-Uniform Mesh Using Local Time Step Method," J. Comput. Phys., **202**, pp. 645–663.
[88] Roache, P. J., 1997, "Quantification of Uncertainty in Computational Fluid Dynamics," Annu. Rev. Fluid Mech., **29**, pp. 123–60.
[89] Najm Habib, N., 2009, "Uncertainty Quantification, and Polynomial Chaos Techniques in Computational Fluid Dynamics," Annu. Rev. Fluid Mech., **41**, pp. 35–52.
[90] DeVolder, B., Glimm, J., Grove, J. W., Kang, Y., Lee, Y., Pao, K., Sharp, D. H., and Ye, K., 2002, "Uncertainty Quantification for Multiscale Simulations," ASME J. Fluids Eng., **124**, pp. 29–41.
[91] Christie, M., Demyanov, V., and Erbas, D., 2006, "Uncertainty Quantification for Porous Media Flows," J. Comput. Phys., **217**, pp. 143–158.
[92] Kulakhmetov, M., Venkattraman, A., and Alexeenko, A., 2010, "Effects of Uncertainty in Gas-Surface Interaction on DSMC Simulations of Hypersonic Flows," 27th International Symposium on Garified Gas Dynamics, July 10-15, CA.
[93] Hadjiconstantinou Nicolas, G., Garcia Alejandro, L., Bazant Martin, Z., and He, G., 2003, "Statistical Error in Particle Simulations of Hydrodynamic Phenomena," J. Comput. Phys., **187**, pp. 274–297.

Downloaded From: http://heattransfer.asmedigitalcollection.asme.org/ on 03/05/2013 Terms of Use: http://asme.org/terms